Reevaluation of the mechanism for ultrananocrystalline diamond deposition from Ar/CH$_4$/H$_2$ gas mixtures

P. W. May,[a)] J. N. Harvey, and J. A. Smith
School of Chemistry, University of Bristol, Bristol BS8 1TS, United Kingdom

Yu. A. Mankelevich
Nuclear Physics Institute, Moscow State University, 119992 Moscow, Russia

Various mechanisms for the growth and renucleation of ultrananocrystalline diamond (UNCD) films are discussed and evaluated in the light of experimental and theoretical evidences in recent publications. We propose that the most likely model for UNCD growth is that where most of the diamond is formed via a similar mechanism to that of microcrystalline diamond films, i.e., gas phase H atoms abstracting surface hydrogens, followed by a CH$_x$, $x=0-3$, addition. Calculations of the gas composition close to the substrate surface in the microwave plasma reactor for both the microcrystalline diamond and the UNCD growth, at substrate temperatures of 1073 and 673 K, suggest that CH$_3$ and C atoms are the most likely precursors for the growth of UNCD. However, the deposition is interrupted by an event which prevents the smooth growth of a continuous layer, and instead creates a surface defect which changes the growth direction and acts as a renucleation site. The possible nature of this event is discussed in detail. Using estimates for reaction rates of various species (including H atoms, Ar* metastables, Ar$^+$ and ArH$^+$ ions) on the diamond surface, a number of mechanisms are discussed and discounted. We propose that the most likely causes for the renucleation required for the UNCD growth are (i) the attachment of C$_1$ species (especially C atoms) followed by local surface restructuring, (ii) the reduction of the efficiency of the β-scission reaction resulting in an increase in the number of long-chained hydrocarbons on the surface, or (iii) a combination of these two processes. © *2006 American Institute of Physics.*
[DOI: 10.1063/1.2195347]

I. INTRODUCTION

Diamond films can be deposited using a chemical vapor deposition (CVD) process involving the gas phase decomposition of a gas mixture containing a small quantity of a hydrocarbon in excess hydrogen.[1] A typical gas mixture uses 1% CH$_4$ in H$_2$, and this produces polycrystalline films with grain sizes in the micron or tens of micron range, depending upon growth conditions, substrate properties, and growth time. The gas mixture can be activated in a number of ways, such as microwave (MW) plasma, combustion torch, or a hot metal filament. The appearance and properties of the microcrystalline diamond (MCD) films produced by each method are very similar, since with all these methods the gas phase chemistry is very similar. This is because the initial reactant gases are converted to approximately the same steady-state mixture of hydrocarbon fragments and hydrogen atoms above the growing surface.[2,3] The Bachmann diagram[4] indicates that due to this similarity in steady-state chemistry, MCD deposition only depends upon the ratios of C:H:O in the input gases and not on their specific chemical identities.

A high concentration of hydrogen atoms close to the substrate surface is crucial in the deposition process, since H performs a number of important functions. First, H atoms can etch surface graphitic (sp^2) carbon many times faster than diamondlike (sp^3-bonded) carbon. Second, the H atoms help to terminate the "dangling bonds" on the diamond surface, thus stabilizing the surface, while growth takes place. Also, the H atoms react with large gas phase hydrocarbon fragments, splitting them into small pieces, thus preventing polymer buildup. Finally, atomic H creates radical sites on the surface by undergoing H-abstraction reactions, removing some of the terminal hydrogens. It is generally believed[5,6] that the main growth species in the standard CVD diamond growth is the CH$_3$ radical, which adds to the diamond surface stepwise following successive hydrogen abstraction by H atoms. Thus, a high concentration of atomic H at the surface is a prerequisite for MCD deposition.

By increasing the ratio of methane in the standard CH$_4$/H$_2$ gas mixture from 1% to ~5%, the grain size of the films decreases and eventually becomes of the order of hundreds down to tens of nanometers. Such nanocrystalline diamond (NCD) films (often termed "cauliflower" or "ballas" diamond) are smoother than the microcrystalline ones, but have larger numbers of grain boundaries that contain substantial amounts of sp^2-bonded carbon impurities. With further addition of CH$_4$, the films become graphitic.

Recently, so-called ultrananocrystalline diamond (UNCD) films have become a topic of great interest, since they offer the possibility of making smooth, hard coatings at relatively low deposition temperatures, which can be patterned to a nanometer resolution.[7] These differ from NCD films, since they have much smaller grain sizes (~3–5 nm), and have a small but non-negligible amount of

---

[a)]Electronic mail: paul.may@bris.ac.uk

sp^2-bonded carbon at atomically abrupt grain boundaries.[8] Most reports of the deposition of these films describe using a microwave plasma CVD reactor and a gas mixture of 1% CH_4 in Ar, usually with the addition of 1%–5% H_2 (which helps to stabilize the lively Ar plasmas). The addition of nitrogen to the plasma during CVD has been found to give the films characteristics that are similar to *n*-type semiconductors, suggesting possible applications in electronic devices. However, the fundamental growth mechanism of these UNCD films is still unclear. Originally, it was suggested[9] that the C_2 radical was the major growth species. However, recent work by us[10] and others[11] have cast doubt on the veracity of this C_2 mechanism. The original reports[12] that UNCD could be grown in a completely hydrogen-free gas chemistry have never been substantiated, and now it is generally agreed that for UNCD deposition to occur, hydrogen atoms must be present in the gas mixture in small amounts (1%–2%), either from decomposition of CH_4 or by addition of H_2. With too little hydrogen present only graphitic films are formed, and with increasing H_2 added the quality of the diamond improves, and there is a transition from UNCD to NCD and then to MCD.[13,14] Indeed, MCD and UNCD can be grown simultaneously in a $CH_4/Ar/H_2$ plasma on different parts of the same substrate.[15] Therefore, it now seems more likely that it is a delicate balance between the concentrations of CH_3 and other gas phase species close to the substrate surface that determines the growth morphology and hence the properties of the resulting film.

II. AIMS AND METHOD

The aim of this paper is to reevaluate the growth mechanism for UNCD based upon recent experimental evidence and to attempt to identify candidate species likely to be important in growth and renucleation. There are two important questions: (1) Which species is responsible for the majority of the carbon which ends up in the nanocrystals; (2) Why do the crystals continually renucleate rather than form larger microcrystals?

The answer to these questions can be obtained if we look at the concentrations of selected gas phase species in the plasma. It is therefore important to use data for species concentrations directly above the growing UNCD surface, as shown in Table I, since species concentrations measured[16] or calculated[17] in the center of the plasma ball will be significantly different due to the far higher temperatures and reaction conditions. The concentrations in Table I have been calculated using a two-dimensional (2D) computer model[18] that has been specifically tailored to the known geometry of our Astex-style microwave CVD reactor, which can deposit UNCD and MCD films using $Ar/CH_4/H_2$ and CH_4/H_2 gas mixtures, respectively. Parameters for the model are taken from experimental observations of the shape and size of the plasma ball in our reactor for different process conditions. For example, an 800 W 1% CH_4/2% H_2/97% Ar plasma at 100 Torr produces a luminous plasma ball that is roughly hemispherical (radius of ~2.5 cm) and positioned ~1 mm above the substrate. The typical temperature of the Si substrate is 1073 K (800 °C), measured by a two-color optical

pyrometer. These process conditions are typical for the UNCD deposition and give an experimental growth rate of ~0.1 μm h^{-1}. By cooling the substrate, UNCD films can be grown at temperatures as low as 673 K (400 °C) at essentially the same rate.

The same sized plasma ball is produced for a 1% CH_4/H_2 gas mixture at 800 W but at a pressure of 20 Torr. For a substrate temperature of 1073 K, this gives a good quality MCD growth with a typical growth rate of 0.3–0.5 μm h^{-1}. But the growth rate and film quality decrease rapidly with substrate temperature so that by 673 K the growth rate is negligible and the film quality entirely graphitic.

A full description of the model will be given in a later paper,[19] but, briefly, the model comprises three blocks, which describe (i) the activation of the reactive mixture (i.e., electromagnetic fields and plasma parameters, power absorption, and gas heating), (ii) gas phase processes (heat and mass transfer and plasma-chemical kinetics), and (iii) gas-surface processes at the substrate. The set of nonstationary conservation equations for mass, momentum, energy, and species concentrations were then solved numerically in cylindrical (r,z) coordinates. Electromagnetic fields (E,H) are not calculated in this approach. Instead, a uniform or weakly nonuniform (~10%) distribution of electron temperature T_e and absorbed power density as a function of T_e and electron density is applied to a hemisphere approximately corresponding to the observed experimental plasma region. For our typical experimental UNCD growth conditions the average input power density is therefore 800 W/33 cm^3 ~ 24 W cm^{-3}. Because of the sharp exponential dependence of ionization rates and electronic densities from the reduced electric field E/N (where N is the gas concentration), a very narrow range of reduced electric fields E/N will be realized in a MW discharge plasma with given input power density levels. We determined the range of E/N for different gas temperatures between 2000 and 4500 K using a zero-dimensional (0D) model for the electron and plasma kinetics. In the 0D model, the balance equations for charged and neutral species are solved for different reduced electric fields. Simultaneously, the electron energy distribution function for the chosen gas mixture composition is calculated by solving the Boltzmann equation in a two-term approximation using a set of known electron-particle collision cross sections.[20] As a result, the steady-state species' number densities and the rate coefficients of electron reactions as a function of T_e are obtained. Typical values of plasma parameters obtained from this model are as follows: $E/N \sim 6.5$–8.5×10^{-17} V^{-1} cm^2, T_e ~2.4–3 eV for a 1% CH_4/2% H_2/97% Ar mixture at 100 Torr, and $E/N \sim 25$–30×10^{-17} V^{-1} cm^2, T_e ~1.3–1.5 eV for a 1% CH_4/H_2 mixture at 20 Torr. Established plasma-chemical mechanisms (~35 species and ~300 reactions for H/C/Ar mixtures)[21–23] together with the electron temperature dependence of the electron collision processes are used in the 2D model of the microwave reactor. The incorporation of nine gas-surface reactions, involving the H abstraction to form surface sites, and the subsequent reactions of these sites with H and hydrocarbon radicals serve to alter significantly the gas composition close to the

TABLE I. Species concentration (cm^{-3}) calculated at a position 1 mm above the substrate surface of the gas phase components present in a MW reactor, for different input gas mixtures and substrate temperatures, that are typical for deposition of UNCD and MCD films in our reactor. The MW power was 800 W and the gas pressure was 100 Torr for the $Ar/H_2/CH_4$ mixture and 20 Torr for the 1% CH_4/H_2 mixture. The values presented in the table are a subset of the full calculated species distributions as a function of distance from the substrate, which will appear in a later paper (Ref. 19). T_{sub} is the substrate temperature, while T_{ns} is the calculated gas temperature near (1 mm from) the substrate surface, which is much lower than in the center of the plasma ball. For some species, excited state concentrations are high enough to be significant, and these are also given in the table. $C_2(a)$ is the 1st excited state of the C_2 radical, $C_2(X)$ is the ground state, CH_2 is the ground state radical, and $CH_2(S)$ is the singlet excited state. Similarly, $H(n=1)$, $H(n=2)$, and $H(n=3)$ are for the ground state and first two excited states of atomic H. Ar^* is the effective level that corresponds to the two lowest metastable levels ($^3P_2$ and $^3P_0$), and Ar^{**} is the two lowest resonance levels ($^3P_1$ and $^1P_1$). $C_xH_3^+$ refers to the total of all the hydrocarbon ions. Also given in the table are the ratios of the concentrations of atomic H, CH_3, and C_2 for the different conditions, as well as the ratio $[C_xH_y]:[H]$, where $[C_xH_y]$ is the total concentration of all hydrocarbon radicals with $x \geq 2$.

	97% Ar/2% H_2/1% CH_4	97% Ar/2% H_2/1% CH_4	1% CH_4/99% H_2	1% CH_4/99% H_2
T_{sub}/K	673	1073	673	1073
T_{ns}/K	2120	2300	1150	1420
H	2.85×10^{15}	5.96×10^{14}	2.72×10^{14}	6.69×10^{13}
CH_3	5.97×10^{11}	8.57×10^{12}	4.10×10^{13}	1.34×10^{13}
C_2H_2	1.68×10^{15}	1.60×10^{15}	3.25×10^{14}	2.62×10^{14}
CH_2	1.97×10^{11}	8.67×10^{11}	2.49×10^{10}	6.32×10^{9}
$CH_2(S)$	1.31×10^{10}	6.29×10^{10}	5.22×10^{8}	1.78×10^{8}
CH	1.32×10^{11}	1.41×10^{11}	2.94×10^{8}	1.91×10^{7}
C	2.12×10^{12}	6.21×10^{11}	2.03×10^{8}	1.67×10^{7}
C_2	7.37×10^{11}	1.94×10^{11}	3.27×10^{6}	4.18×10^{6}
$C_2(X)$	1.43×10^{11}	2.26×10^{10}	9.44×10^{4}	4.39×10^{4}
C_2H	9.15×10^{12}	3.93×10^{12}	3.19×10^{9}	1.93×10^{9}
C_2H_3	3.38×10^{10}	1.42×10^{10}	9.11×10^{10}	6.01×10^{9}
C_2H_4	1.70×10^{10}	6.20×10^{10}	5.67×10^{12}	1.38×10^{12}
C_2H_5	7.86×10^{5}	3.70×10^{8}	1.50×10^{10}	2.44×10^{9}
C_2H_6	1.50×10^{5}	2.67×10^{7}	1.01×10^{12}	3.35×10^{10}
H_2	1.46×10^{16}	1.54×10^{16}	1.31×10^{17}	1.05×10^{17}
CH_4	1.57×10^{11}	1.02×10^{13}	8.66×10^{14}	6.68×10^{14}
C_3	1.80×10^{14}	4.09×10^{13}	1.07×10^{10}	8.26×10^{8}
C_3H	8.07×10^{11}	5.69×10^{11}	6.72×10^{8}	1.75×10^{8}
C_3H_2	3.63×10^{13}	1.28×10^{14}	3.04×10^{12}	2.32×10^{12}
C_4	1.75×10^{10}	1.89×10^{9}	7.57×10^{1}	2.62×10^{1}
C_4H	2.54×10^{11}	1.10×10^{11}	1.25×10^{5}	1.34×10^{5}
C_4H_2	3.42×10^{13}	4.51×10^{13}	1.48×10^{11}	9.09×10^{10}
$H(n=2)$	1.99×10^{10}	5.46×10^{9}	2.01×10^{8}	4.17×10^{7}
$H(n=3)$	3.76×10^{8}	1.37×10^{8}	2.55×10^{5}	5.04×10^{4}
Ar^*	1.30×10^{11}	1.81×10^{11}	...	...
Ar^{**}	1.96×10^{10}	2.35×10^{10}	...	...
Electrons	3.37×10^{12}	3.57×10^{12}	2.51×10^{11}	2.01×10^{11}
$C_xH_y^+$	2.189×10^{12}	3.40×10^{12}	2.48×10^{11}	1.98×10^{11}
H_3^+	2.05×10^{10}	8.13×10^{9}	3.69×10^{9}	3.15×10^{9}
H_2^+	3.20×10^{5}	5.01×10^{5}	2.52×10^{6}	2.04×10^{6}
ArH^+	4.55×10^{11}	1.57×10^{11}	...	...
Ar^+	8.53×10^{7}	1.18×10^{8}	...	...
Ar	4.35×10^{17}	4.00×10^{17}	...	...
Ratios				
$[H]:[CH_3]$	4774	69.5	6.6	5.0
$[H]:[C_2]$	3239	2752	8.3×10^{7}	1.6×10^{7}
$[CH_3]:[C_2]$	0.68	39.6	1.2×10^{7}	3.2×10^{6}
$[C_xH_y]:[H]$	0.092	0.333	0.012	0.036
Film type	UNCD	UNCD	No film or graphitic	MCD

surface. Our model has a spatial resolution of 1 mm, and so we are assuming that the species concentrations that are calculated 1 mm from the surface are representative of those at the growing diamond surface itself.

Two tests show that this model gives what appears to be a realistic description of the plasma processes. First, the cal-

culated number density for the C_2 radical in the *center* of the plasma ball for a 1% CH_4/2% H_2/97% Ar gas mixture (100 Torr, 800 W) is $\sim 5 \times 10^{13}$ cm^{-3}, which agrees closely with experimental measurements from similar plasmas.[17] Second, the calculated gas temperature in the center of the plasma is 3900 K, dropping to ~ 2300 K close to the sub-
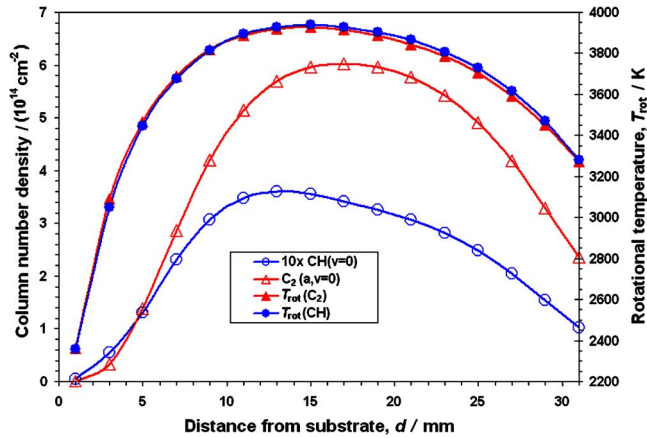
FIG. 1. (Color online) Calculated column densities and rotational temperatures of CH and $C_2(a)$ at different distances from the substrates for a MW reactor operating at 800 W and a pressure of 100 Torr with a gas mixture of 1% CH_4/2% H_2/Ar. Note that the T_{rot} values in the center of the plasma of ~3900 K are the values that would be measured by a line-of-sight absorption technique such as cavity ring down spectroscopy. These values are close to the gas temperatures and values of T_{rot} measured by optical emission spectroscopy (e.g., temperature fitting the band contour of the C_2 Swan band).

strate (see Fig. 1). This is consistent with measurements of the gas temperature (usually taken from rotational temperatures of C_2) in similar Ar/CH_4/H_2 plasmas.[10,16,17] Although we calculate the concentrations of all the major neutral and ionic species as a function of position within the plasma, Table I only shows a subset of these data for these species concentrations immediately above (1 mm) the growing UNCD surface. The full 2D concentration profiles will appear in a later paper.[19]

III. RESULTS AND DISCUSSION

A. The "growth species"

Comparing the data in columns 2 and 4 (T_{sub}=1073 K) in Table I, it is clear that when the gas mixture changes from 20 Torr 1% CH_4/H_2 (MCD growth conditions) to 100 Torr 1% CH_4/2% H_2/Ar (UNCD growth conditions), the absolute concentration of H atoms increases by a factor of ~9, while the concentration of methyl stays approximately the same. Thus, both H and CH_3 are still in relatively high proportion compared to almost all the other reactive gas phase species (except for C_2H; see below). We note that [C_2] is calculated to be 40 times less than [CH_3] for standard UNCD growth conditions, a concentration that makes it unlikely to account for the observed deposition rate of UNCD. Furthermore, the measurements of Rabeau *et al.*[11] show that changes in [C_2] in the plasma do not mirror the observed UNCD growth rates, and their conclusion was that C_2 could not be the major growth species. The C_2H radical, however, is present in much higher concentration at the growth surface (comparable to that of CH_3), and therefore, is a much more likely candidate growth species than C_2. However, no experimental or theoretical work has yet been performed on the reactivity of C_2H with diamond surfaces, and so its effectiveness as a growth species remains unclear.

The ability of UNCD to be deposited at low substrate temperatures (673 K) (Ref. 7), which implies a lower activation barrier for growth, might suggest that there is a different growth mechanism to that from MCD. But a lower activation barrier does not necessarily imply a completely different growth mechanism—only that *one* (rate limiting step) out of the many steps leading to the growth has a lower barrier. The H abstraction and/or addition of CH_3 to a spherical nanograin, where the surface consists almost entirely of atomically rough steps and edges, might easily be more efficient and so have different energetics and kinetics from those on flat crystal surfaces. Furthermore, MCD (albeit poor quality) can be grown at substrate temperatures as low as 600 °C using conventional CVD gas mixtures (e.g., CO_2/CH_4);[24] so for UNCD to be grown at temperatures only 150 °C colder is not, in our opinion, sufficient evidence for a different diamond growth mechanism based on different precursors (C_2 or C_2H).

Although a growth mechanism based on C_2 or C_2H precursors cannot be entirely ruled out at this stage, based on the arguments above and the other experimental evidence mentioned in the Introduction, it is not unreasonable to suggest that the UNCD growth proceeds along much the same lines as the MCD growth, with a mechanism based on H abstraction followed by the addition of C_1 species. For H-rich conditions and/or high temperatures, the species added would be primarily CH_3. But for Ar/CH_4 gas mixtures, other C_1 species, such as CH_2, CH, and C might also add to the surface. The addition of most of these species would propagate the diamond lattice as before. But the difference is that the addition of any of these other C_1 species would create a highly reactive surface site having two or three dangling bonds on the same site. This high energy site can either (a) add H's reterminating the diamond surface as normal or (b) reorganize the surface forming nondiamond structures, or (c) react with any nearby gas phase species (including C_2, C_2H, etc.), forming a surface defect. Both (b) and (c) would provide suitable renucleation sites necessary to explain the nanocrystal growth. Since [H] is much greater than the concentration of other hydrocarbon radical species, process (a) will dominate, and so growth from any of these C_1 species would be almost identical to, and indistinguishable from, growth by methyl addition. The crucial difference is that there is now the small possibility that the relatively improbable processes (b) and (c) produce a surface defect. This seems to be consistent with the observed features of the UNCD growth, namely, the formation of nanosized crystals as a result of relatively rare renucleation events.

If this mechanism is true, then the majority of the carbon in the nanocrystals would originate from a combination of CH_3 and other C_1 species. For this proposed mechanism, it is possible to estimate the contribution to the growth rate G (in μm h^{-1}) of the important C_1 species, using formulas derived in Ref. 25:

$$G_{CH_3} = 3.8 \times 10^{-14} T_{ns}^{0.5}[CH_3]/(1 + k_2/k_1)^2, \quad (1)$$

TABLE II. Rate coefficients used in the site fraction calculations in Fig. 2 for a 1% CH_4/2% H_2/Ar plasma, calculated (Ref. 25 and 26) from $k_1 = 3.2 \times 10^{-12} N_A T_{ns}^{0.5} \exp(-3430/T_{sub})$, $k_2 = 9.6 \times 10^{-13} N_A T_{ns}^{0.5}$, where T_{sub} is the substrate temperature (1073 K), T_{ns} is the gas temperature near (1 mm from) the substrate (which from Table I is 2300 K) and N_A is Avogadro's number. k_{-1} and k_3 are from Refs. 29 and 43 and references therein.

	Rate coefficient $(mol^{-1}\ cm^3\ s^{-1})$
k_1	3.78×10^{12}
k_2	2.77×10^{13}
k_3	1×10^{13}
k_{-1}	1600

$$G_{CH_x} = 3.9 \times 10^{-14} T_{ns}^{0.5}[CH_x]/(1 + k_2/k_1), \quad (2)$$

where T_{ns} is the gas temperature near the substrate and CH_x is for $x = 0, 1, 2$. k_1 and k_2 are the rate constants for surface H abstraction and addition and are defined in reactions (R1) and (R2), below. Values for k_1 and k_2 (in units of $mol^{-1}\ cm^3\ s^{-1}$) can be calculated following the procedure outlined by Krasnoperov *et al.*,[26] (see Table II). Using these values and the calculated T_{ns} values and species concentrations from Table II, we have obtained growth rates (Table III) for 1073 K (a typical growth temperature for both MCD and UNCD) and 673 K (the lowest temperature for which a UNCD growth has been reported). The calculated values for both gas mixtures and temperatures are comparable with our own experimental growth rates as well as with published results.[11,14] It is clear that for MCD diamond growth conditions, CH_3 can account for almost all of the deposited films at standard growth temperatures, while at low temperatures the growth rate falls to almost zero. But for UNCD growth conditions, all the C_1 precursors contribute in varying amounts to the growth, depending on substrate temperatures. At high T_{sub}, the contributions to the growth from CH_3, CH_2, and C atoms are almost equal. At low T_{sub} growth is much slower and is dominated by C atoms.

The reason for the shift from the CH_3 growth to the growth from other C_1 species in Ar/CH_4/H_2 plasmas can be rationalized, since in a MW reactor under the conditions necessary for the UNCD growth, the hot plasma region extends to within a very small distance from the substrate.[27] Thus, all the C_1 species, not just CH_3, have high concentrations just above the substrate surface, even for low substrate temperatures ~673 K. Note that such conditions are never realized in typical hot filament CVD (HFCVD), since the gas temperature near the surface is only $T_{ns} \sim T_{sub} + 100$ K. This means that there is a very low concentration of C_1 species at the surface, and the only growth precursor, CH_3, rapidly decreases in concentration with lower substrate temperatures because of the reaction $CH_3 + H + M \rightarrow CH_4 + M$. Thus, the prediction is that UNCD film growth *might* be possible in HFCVD, so long as the substrate temperature is high enough, but low temperature HFCVD of UNCD would not work. Experimental evidence for this is that NCD and UNCD film growth have been reported for high substrate temperatures with[28] and without[27] dc plasma assistance, but there are no reports of a low temperature HFCVD UNCD growth.

B. The renucleation species

If UNCD grows by the same general reaction steps as MCD, the important question then becomes: What makes the diamond continually renucleate? To make ~5-nm-diameter grains (containing about 12 000 carbon atoms), on average, after every 12 000 methyls (or other C_1 species) are added to the surface, an "event" occurs which interrupts the smooth growth process, causing a surface defect or reconstruction and leading to the renucleation of a crystallite with a different growth direction and/or morphology from that of its parent. The identification of this event would go a long way to elucidating the mechanism for the UNCD growth. One possible such event was outlined earlier, namely, that if a C_1 radical adds to the surface and forms a high energy defect with two or three dangling bonds, this would provide a site for renucleation. However, there are other possibilities worth investigating.

To gain an insight into the differences between MCD and UNCD growth processes, we shall follow the kinetic approach outlined by Butler and Goodwin.[29] The generally accepted growth steps for the MCD film growth include the following three basic reactions, to which we have added a further reaction (R4) to include C_1 species other than methyl:

$$H + C_dH \rightarrow C_d + H_2 \quad [\text{Reaction 1 (R1)}],$$
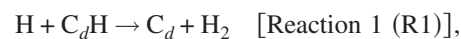
TABLE III. Calculated film growth rates G for possible C_1 growth precursors for high and low temperature MCD and UNCD growth conditions. The values for CH_3 were calculated using Eq. (1) in the text, and for the other three precursors using Eq. (2). [Note that we are assuming that CH_2 adds to a single site, as for C and CH. If it adds to a biradical site, Eq. (1) needs to be used instead, and the values for $G(CH_2)$ become ~10× lower than those in the table]. It is clear that for the CH_4/H_2 gas mixture, growth is dominated by CH_3 at high T_{sub}, while at low T_{sub} growth rates are very low. But for Ar/CH_4 gas mixtures, all the C_1 precursors contribute in varying amounts to the growth depending on temperature. At high T_{sub}, the contributions to the growth from CH_3, CH_2, and C atoms are almost equal. At low T_{sub} growth is much slower and dominated by C atoms.

	"Growth" precursor			
Calculated growth rate ($\mu m\ h^{-1}$)	CH_3	CH_2	CH	C
G ($T_{sub} = 673$ K, 1% CH_4/99% H_2)	0.02	6×10^{-4}	8×10^{-4}	5×10^{-6}
G ($T_{sub} = 1073$ K, 1% CH_4/99% H_2)	0.27	0.001	3×10^{-6}	3×10^{-6}
G ($T_{sub} = 673$ K, 97% Ar/2% H_2/1% CH_4)	3.9×10^{-4}	0.007	0.005	0.074
G ($T_{sub} = 1073$ K, 97% Ar/2% H_2/1% CH_4)	0.22	0.20	0.03	0.14

$$H + C_d \rightarrow C_dH \quad [\text{Reaction 2 (R2)}],$$

$$C_d + CH_3 \rightarrow C_dCH_3 \quad [\text{Reaction 3 (R3)}],$$

$$C_d + CH_x \rightarrow C_dCH_x, \quad x = 0-2 \quad [\text{Reaction 4 (R4)}],$$
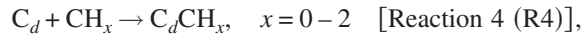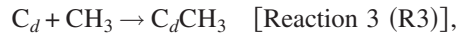
where C_d refers to a diamond surface with an open site or dangling bond and C_dH is a hydrogen terminated surface. Reaction (R1) is the abstraction of a terminating hydrogen by a gas phase H atom, producing a reactive surface radical site. Reaction (R2) is the addition of a H atom to the surface radical site, thereby returning the diamond surface to its normal hydrogen terminated state. The excess energy from the bond formation process generates surface heating and contributes to the high substrate temperature. Reaction (R3) is the "growth step," whereby gas phase CH_3 adds to the surface. Subsequent H-abstraction reactions and CH_3 additions serve to propagate the diamond lattice (see Ref. 29 for more details). According to Skokov *et al.*,[30] the incorporation (rather than adsorption) of CH_3 into the diamond requires a biradical site (two adjacent open sites).

Reaction (R4) becomes important only under conditions where the concentrations of the CH_x ($x < 3$) radicals become non-negligible compared to $[CH_3]$ and $[H]$, as is the case for the UNCD growth. We assume that C, CH, and CH_2 could be incorporated into the diamond on isolated open sites. Thus, the growth rate due to CH_x ($x < 3$) will be proportional to the C_d fraction rather than to C_d^2, as is the case for the methyl growth. These assumptions are reflected in growth rate expressions (1) and (2). The rate constants for the forward reactions are given by k_1, k_2, k_3, and k_4, and for the reverse reactions by k_{-1}, k_{-2}, k_{-3}, and k_{-4}.

For normal H-rich CVD diamond deposition conditions, all three forward reactions [(R1)–(R3)] are fast and are in steady-state, and we can ignore reaction (R4). If we assume that the rate of the H abstraction ($k_1[H][C_dH]$) is much greater than the rate at which methyl desorbs, ($k_{-3}[C_dCH_3]$), i.e., the reverse of reaction (R3), and if we apply steady state to $[C_d]$ we get that the fraction of open sites is given by

$$\frac{[C_d]}{[C_dH] + [C_d]} = \frac{k_1[H]}{k_1[H] + k_2[H] + k_{-1}[H_2] + k_3[CH_3]}. \quad (3)$$

For typical CVD diamond conditions, $k_{-1}(H_2) \ll k_2[H]$; so the equation is reduced to

$$\frac{[C_d]}{[C_dH] + [C_d]} \approx \frac{k_1}{k_1 + k_2 + k_3[CH_3]/[H]} \quad (4)$$

since k_2 is comparable in magnitude to k_3, and the methyl concentration is usually less than the H concentration, so that $k_3[CH_3] < k_2[H]$. Therefore, Eq. (4) is simplified to

$$\frac{[C_d]}{[C_dH] + [C_d]} \approx \frac{k_1}{k_1 + k_2}. \quad (5)$$

This means that so long as there is a sufficiently high ratio of [H] to $[CH_3]$, i.e., above $\sim 5:1$, the fraction of open sites remains constant at around 12% (see Fig. 2), but this will increase rapidly with temperature through the temperature dependence of k_1.
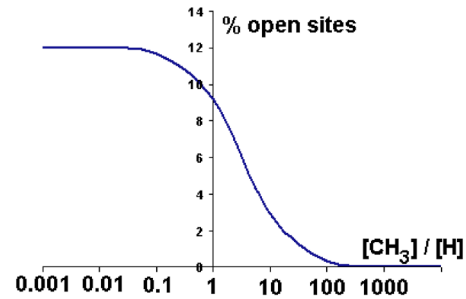
FIG. 2. (Color online) The percentage of open sites on a diamond surface as a function of $[CH_3]:[H]$ ratio, as calculated from Eq. (4) at a substrate temperature of 1073 K.

C. Renucleation due to excess open surface sites

One suggestion for a possible mechanism to produce renucleation on the surface is if the number of open sites (dangling bonds) becomes too high. If two open sites were formed adjacent to each other, there might be the possibility of cross linking or surface reconstruction, which would break the symmetry of the lattice and perhaps be an ideal site for renucleation. If this second layer were to start growing before the first layer were complete, we would end up with pyramids or islands, which might ultimately lead to nanocrystallites. Let us now consider some candidate species and processes which may be responsible for producing an excess of open sites, and discuss if their concentrations and reaction rates are feasible for renucleation.

1. Excess H atoms

From Table I it is clear that on going from MCD to UNCD growth conditions the ratio of $[H]:[CH_3]$ increases significantly, especially at low substrate temperatures. It has been suggested that this excess H atom concentration might be responsible for an increased number of open sites. But from Fig. 2, we can see that this cannot be true, since the $[H]:[CH_3]$ is such that the fraction of open sites has already reached a saturation level of $\sim 12\%$, as given by Eq. (5).

2. Ar containing species

Additional open sites might be created if one of the other species in the gas phase (apart from H) were to abstract surface hydrogens at a sufficiently high rate. Thus, we may add another basic reaction to the ones mentioned above, for a generic species, X:

$$X + C_dH \rightarrow C_d + X + H \quad \text{or} \quad C_d + X - H$$

$$[\text{Reaction 5 (R5)}].$$
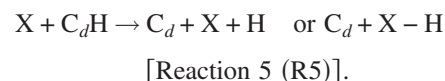
This will have forward and backward rate constants of k_5 and k_{-5}, respectively (with k_5 assumed to be much greater than k_{-5}). As before, assuming that $(k_1[H][C_dH]) \gg (k_{-3}[C_dCH_3])$, and also that $k_3[CH_3] < k_2[H]$, applying steady state to $[C_d]$ gives the fraction of open sites as being

$$\frac{[C_d]}{[C_dH] + [C_d]} = \frac{k_1 + k_5[X]/[H]}{k_1 + k_2 + k_5[X]/[H]}. \quad (6)$$

This is reduced back to Eq. (5) for small $[X]$, as expected. Therefore, the two important parameters which control

whether reaction (R5) is a significant process are the concentration of X close to the surface and its rate of H abstraction, k_5. Thus, we now consider the predictions of this equation for different species, X.

a. Ar^* metastables. The first species to consider is X=Ar^*, since the two $4s$ metastable states of Ar have 11.5 and 11.7 eV of energy and lifetimes of milliseconds. These species can survive long enough to diffuse to and interact with the diamond surface. If they were to donate some or all of their energy to the surface, there would easily be sufficient energy to break a C–H bond (4.4 eV) or to cause a Penning ionization via

$$Ar^* + C_dH \rightarrow C_dH^+ + Ar + e \quad [\text{Reaction 6 (R6)}],$$

with rate constant k_6 (being the specific case of the general rate constant k_5), possibly leading to a subsequent surface reconstruction. Table I shows that $[Ar^*]$ under UNCD growth conditions is $\sim 10^{11}$ cm^{-3}, which is 10^3 times lower than that of H. The value for k_6 is not known for Ar^*; however, rate constants for analogous reactions of argon metastables with molecules such as methane or ethane have been measured and are large,[31] typically of the order of 10^{13} mol^{-1} cm^3 s^{-1}. Most often, the reaction leads to the breaking of one or several C–H bonds by dissociative energy transfer (as in R5), but dissociative Penning ionization (equivalent to R6 followed by loss of H$^+$) is possible also. However, using Eq. (6) with the calculated concentrations for H and Ar^* and the estimate for $k_6(=k_5)$ mentioned above gives an insignificant change in the fraction of open sites. Thus, we can rule out Ar^* metastables as being a cause of extra surface sites.

b. Ar^+ ions. Since Ar^+ is an ionic species and Ar has a large ionization energy, there is the possibility of a thermal electron transfer process from the surface, probably accompanied by C–H bond dissociation, creating a surface ion:

$$Ar^+ + C_dH \rightarrow C_d^+ + Ar + H \quad [\text{Reaction 7 (R7)}].$$
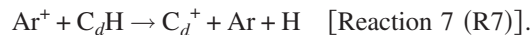
But from Table I, the concentration of Ar^+ is only 10^8 cm^{-3}, so the rate constant k_7 would have to be extremely large for this process to play a significant role. The nearest analog is an electron transfer from small gas phase molecules. The cross section for a dissociative electron transfer upon collision of Ar^+ with acetylene[32] is equivalent to a rate constant of the order of 10^{13} mol^{-1} cm^3 s^{-1}. Using these values in Eq. (6) shows that thermal Ar^+ ions can also be ruled out as candidates for surface site creation.

c. ArH^+. From Table I, the concentration of ArH^+ is $\sim 10^{11}$ cm^{-3}, far higher than that of the other ions in the plasma, which makes it a potential candidate for renucleation. ArH^+ is a strong acid, which can transfer a proton to neutral molecules such as H$_2$ or methane,[33] with a rate constant of the order of 10^{13} mol^{-1} cm^3 s^{-1}. An analogous reaction with the diamond surface is shown as (R8):

$$ArH^+ + C_dH \rightarrow C_dH_2^+ + Ar \rightarrow C_d^+ + Ar + H_2$$
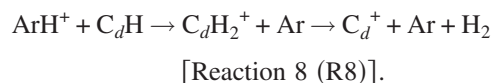
$$[\text{Reaction 8 (R8)}].$$

ArH^+ could also transfer an electron from the surface, leading to argon and hydrogen atoms. Using 10^{13} mol^{-1} cm^3 s^{-1} as an estimate for the forward rate of reaction (R8), k_8, we find that the fraction of open sites is, again, not significantly changed by this extra mechanism.

d. Excited H atoms. ArH^+ can also dissociate on the surface to produce Ar and excited H atoms, where H will be in the $n=2$ or greater state. Highly excited H that is created right at the substrate surface may also play a role in surface renucleation. But Table I shows that the concentration of excited H($n=2$) is only $\sim 10^9$ cm^{-3}, which makes it unlikely to be a significant factor in surface reactions.

D. Insertion reactions

1. C_2 insertion

Molecular dynamics calculations have shown that the C$_2$ radical can incorporate into the hydrogenated (110) surface[34,35] and also into the hydrogen-free (110) surface[36] of the growing diamond by a low barrier insertion mechanism. Such insertions would certainly disrupt the lattice, leading to a change in the growth direction. Under UNCD growth conditions [C$_2$] close to the surface is only 2×10^{11} cm^{-3} (sum of ground state and first excited state, from Table I), which is 40 times less than that of CH$_3$. Thus, for a nanograin containing $\sim 12\,000$ C atoms, a sticking probability for C$_2$ of only (40/12 000) 1 in 300 is all that would be required to produce a renucleation event resulting in 5 nm crystallites, which at first sight seems reasonable. However, since the C$_2$ insertion mechanism has a low energy barrier only for certain diamond lattice planes[37] and not for others, it would be expected that this would lead to preferentially oriented microcrystal or even macrocrystal growth. But UNCD crystals are essentially spherical, with no apparent preferred orientation. This suggests that perhaps C$_2$ is not the most important species responsible for renucleation.

2. C_2H insertion

One species that has been largely ignored in the UNCD literature is C$_2$H. This is because it does not emit visible light under standard plasma growth conditions and is difficult to detect by other spectroscopic means. However, its concentration close to the surface is very large compared to the other reactive radicals (see Table I). It has a concentration 20 times higher than that of C$_2$ (for $T_{sub}=1073$ K) and is comparable with that of CH$_3$. No calculations or measurements have yet been reported as to the reaction rate of C$_2$H with a diamond surface; however, if we make the assumption that it will react similarly to C$_2$, then this looks like a very good candidate for the renucleation species, since it would have both a high reaction rate k_5 and a sufficiently high concentration. However, if it behaves like C$_2$, then C$_2$H insertion, too, should produce a preferentially orientated growth, leading to large microcrystallites, contrary to experimental observations.

E. Reduction in β-scission efficiency

Larger hydrocarbon species can also add to the surface by a reaction such as (R9).
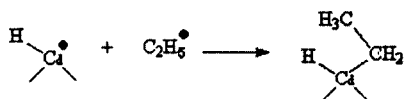
[**Reaction 9 (R9)**]

but they are normally rapidly removed from a growing MCD surface by β-scission reactions, such as
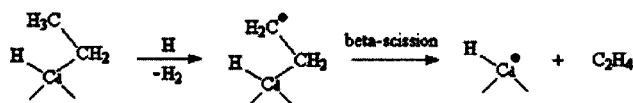
[Reaction 10 (R10)]
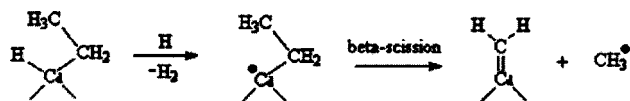
[Reaction 11 (R11)]

High concentrations of long hydrocarbon radicals will favor (R9), whereas high concentrations of H atoms will favor (R10) and (R11). The proportion of long-chained hydrocarbon radicals to that of H atoms will determine the relative efficiencies of these three reactions. For UNCD conditions, the concentrations of larger hydrocarbons becomes nonnegligible (see Table I), and so it is possible that C_2H, C_3, C_4, and other C_xH_y ($x \geq 3$), which have significant concentrations near the growth surface, may survive for longer on the surface before being finally removed back into the gas phase. During the time that these species are "blocking" a surface site, they will interrupt the normal diamond growth process at adjacent sites, possibly leading to a change in growth characteristics.

If the relative proportion of higher hydrocarbons to atomic H increases further, then the probability of two hydrocarbon species being adjacent to each other becomes *nonnegligible*. We then have the possibility of cross linking and the formation of graphitic impurities, as is believed to be the case for NCD cauliflower films grown with high methane concentrations (e.g., 4% CH_4/H_2). The fact that UNCD films contain little graphitic materials at the grain boundaries suggests that this latter process does not occur. However, an inhibited or slowed β-scission reaction might very well account for a renucleation rate of 1 in 12 000 required to explain the UNCD grain size. To try to quantify this, we can add two more potential reactions for the addition to the diamond surface of a large hydrocarbon *radical* species C_xH_y with $x \geq 2$, and then its subsequent removal via a β-scission reaction:

$$C_d + C_xH_y \rightarrow C_dC_xH_y \quad \text{[Reaction 12 (R12)]},$$

$$C_dC_xH_y + H \rightarrow C_d + C_xH_{y+1} \quad \text{[Reaction 13 (R13)]},$$
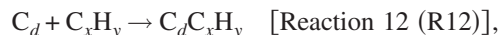
with forward and backward rate constants of k_{12}, k_{-12} and k_{13}, k_{-3}, respectively. Note that C_xH_y includes both C_2 and C_2H as well as higher hydrocarbons. We shall assume that the backward reaction rates are slow compared to the forward rates, and so can be ignored. Applying a steady state to the concentration of surface sites occupied by large hydrocarbon species $[C_d\text{-}C_xH_y]$, we obtain

$$k_{12}[C_d][C_xH_y] = k_{13}[C_dC_xH_y][H], \quad (7)$$

and since for UNCD growth conditions [H] is beyond the saturation threshold, so that the total fraction of open sites is given by Eq. (5), we get that the fraction of the filled sites that are actually occupied by large hydrocarbons is

$$\frac{[C_dC_xH_y]}{[C_dH]} = \frac{k_1}{k_2}\frac{k_{12}[C_xH_y]}{k_{13}[H]} = k'\frac{[C_xH_y]}{[H]}. \quad (8)$$

As expected, Eq. (8) reduces to zero for large [H] or small $[C_xH_y]$, i.e., MCD growth conditions. For plasma conditions with smaller [H] and/or larger $[C_xH_y]$, then the fraction of sites filled by large hydrocarbon molecules becomes a function of the ratio of the two concentrations $[C_xH_y]:[H]$. Many hydrocarbon fragments such as C_2H, C_2H_3, and C_3H are expected to form strong bonds to surface radical sites, so that k_{12} would be large—similar in magnitude to the rate constant k_3 for the analogous addition of methyl radicals. k_{-12} would be small enough to ensure a significant lifetime for the surface-bound hydrocarbon fragment. The etching process (R13) will have rate constants depending on the structure of the hydrocarbon fragment, and at least in some cases might be small enough to lead to long-lived surface fragments. In the absence of any experimental measurements, a reasonable estimate for k_{13} would be to say that the etching process is generally similar to that of reaction (R1), so $k_{13} \sim k_1 = 3.85 \times 10^{12}$ mol^{-1} cm^3 s^{-1}. From Table I, the value of $[C_xH_y]:[H]$ for the MCD growth conditions is 0.036, but for UNCD growth conditions, the ratio becomes 0.333, i.e., ten times larger. Using Eq. (8) with these ratio values, plus the above estimates for k_{12} and k_{13}, we calculate that for MCD growth conditions the steady-state fraction of sites that are occupied by large hydrocarbons is $\sim 1\%$, and so the surface may be considered to be almost free of long-chained hydrocarbons. But for UNCD growth conditions, this fraction is $\sim 12\%$, and so the surface sites now contain significantly more longer-chained hydrocarbons. Thus, it seems feasible that a reduction in the efficiency of the β-scission reactions could lead to the disruption of the growth that is required for nanograin formation.

Indirect evidence for this comes from the observation of the 1150–1170 cm^{-1} line in Raman spectroscopy which is a characteristic of UNCD films and which has been assigned to long-chained sp^2-bonded carbon molecules, such as *trans*-polyacetylene, present at the grain boundaries.[38] To date, there has been no satisfactory explanation suggested for the presence of these molecules. A decrease in the β-scission reaction efficiency, as proposed above, might be one mechanism by which longer hydrocarbon molecules could begin to grow at the diamond surface, to be subsequently trapped in a grain boundary as the neighboring grain encroaches.

F. Ion bombardment

As well as thermal ions diffusing to and reacting with the surface, as discussed above, another possibility is that ions from the plasma can be accelerated onto the growing diamond surface and impact with sufficient kinetic energy to break bonds and cause surface reconstruction.[39] It is known that when an external bias of a few 100 V is applied during

deposition, the ion bombardment of the growing diamond leads to a reduction in the crystallite size, or even to amorphization.[40] But in the absence of any external bias, the sheath potential at the grounded substrate surface in a MW plasma will be approximately equal to the floating plasma potential, since even if the substrate is sitting on an electrically grounded holder the diamond film will be insulating and so the surface will be effectively floating. The magnitude of the sheath potential can be estimated using equations in Ref. 41 for typical MW plasma conditions to be a few tens of volts, and in high power, high temperature MW it may reach as high as 100 V. However, at pressures of >100 Torr the ions will experience many collisions within this sheath region. A typical mean free path for an Ar^+ ion at 100 Torr is ~ 25 μm, which is much smaller than the sheath thickness, which is typically ~ 0.5 mm. If we assume that, on average, an ion loses approximately 50% of its kinetic energy from each collision, then it will only take three or four collisions to reduce the ion energy to below that required to break a chemical bond, say, 2 eV. Collisional energy losses will therefore be significant, and the ions can be considered to be effectively thermalized. Thus, the ions will impact the surface with kinetic energies insufficient to affect the growth process in any significant way.

Reactor designs are beginning to use large areas and higher applied MW powers, but also higher pressures. These will change the electron temperature, the sheath thickness, and the collision rates in the plasma, and hence alter the ion bombardment energies. For very high power reactors, therefore, ion bombardment effects may become non-negligible and may warrant further study.

Evidence against ion bombardment being a significant factor in the UNCD formation comes from two papers that report the growth of NCD films using hot filament (HF) reactors, in which there should be nominally no ions, and hence no ion bombardment. Lin *et al.*[28] reported a growth of films from an $Ar/CH_4/H_2$ gas mixture in a hot filament reactor and found the gas composition range for which UNCD-like films were deposited. The transmission electron microscopy (TEM) images of the films showed nanosized grains with sharp grain boundaries and a very smooth film surface, and were convincingly similar to those of UNCD. However, they also say they used an external dc bias to enhance the growth rate and to allow the observation of the C_2 emission lines, especially at high Ar concentrations. It was unclear from their paper whether this bias was necessary to make UNCD films, or whether absence of the bias resulted in NCD or no growth. A later paper by our own group[27] extended their $Ar/CH_4/H_2$ composition diagram and also focused more on the small range of gas compositions which produced UNCD-like film growth using an unbiased HF reactor. The films were smooth with submicron grain sizes and gave the typical Raman spectrum characteristic of UNCD (including the 1150 cm^{-1} peak). However, no TEM results were presented to show conclusively that the films were UNCD as opposed to a NCD or a cauliflower diamond. Clearly, more work needs to be done in this area, since if true UNCD films can be deposited in a nominally ion-free HF reactor with no

external bias, then ion bombardment can be ruled out as a significant mechanism for nanograin formation in these films.

G. Thermodynamic stability

One intriguing possibility to explain the formation of UNCD films comes from a recent paper by Raty and Galli,[42] who suggested that the size distribution of UNCD could be explained simply by thermodynamic stability considerations. They carried out *ab initio* calculations on the stability of a nanodiamond as a function of surface hydrogen coverage and grain size. They found that for a broad range of pressures and temperatures, particles with bare, reconstructed surfaces become thermodynamically more stable at a size of ~ 3 nm than those with hydrogenated surfaces. This stability prevents the formation of larger grains. The $2-3$ nm clusters consist of a diamond core surrounded by a fullerenelike carbon network and have been termed "bucky diamonds."[43] The type of film that is grown would depend upon the temperature and concentration of H, with lower temperatures and higher concentration favoring MCD growth, while the converse favors UNCD growth. The low H content in the UNCD films and the 2%–5% sp^2 carbon present at the grain boundaries (as evidenced by the prominent D peak seen in Raman spectra from UNCD films, plus the previously mentioned 1150 cm^{-1} Raman line) provide experimental evidence that the nanodiamond crystals do have nondiamond carbon at the grain boundaries.

Although intriguing, there are a number of problems with this model. First, UNCD films can be grown onto single crystal diamond substrates, but the theory says that growth on "infinite" smooth diamond surfaces should produce MCD or epitaxial diamond. But more importantly, the H concentration in the $Ar/CH_4/H_2$ gas mixtures is only a factor of 3 different to that in the CH_4/H_2 mixtures, which should not be sufficient to justify a change in growth morphology. Furthermore, UNCD can also be grown at essentially the same rate at both high (1073 K) and low (673 K) substrate temperatures, which contradicts the predictions of this model. Thus, the model may go some way in explaining why, once formed, the UNCD grains remain stable, but it does not explain why they form in the first instance.

IV. CONCLUSIONS

In this paper we have reviewed many possible candidate species and processes that might be responsible for the characteristic growth of UNCD. We have discussed the pros and cons of each in turn, with the aim of identifying plausible growth mechanisms that are consistent with all the published evidence, and also to highlight the areas in which there is a lack of knowledge and which therefore require further study.

Based on the arguments given above, we believe that UNCD grows via a mechanism similar to that for MCD, namely, the surface H abstraction by gas phase H atoms, followed by the addition of a C_1 species. For the MCD growth with gas mixtures containing high concentrations of H_2 and high substrate temperatures, the C_1 species is predominantly CH_3. But for lower substrate temperatures or

lower hydrogen concentrations, as in $Ar/CH_4/H_2$ gas mixtures, growth occurs via the addition of all C_1 species, CH_3, CH_2, CH, and atomic C, which contribute in varying amounts depending on growth conditions. Since [H] at the surface is still relatively high, even in so-called H-poor plasmas, the C_1 species attached to the diamond surface will be rapidly hydrogenated to CH_2 or CH_3. Thus, the subsequent mechanism would be hard to distinguish from growth by CH_3. However, there is a small but nonzero probability that the highly reactive C_1 species on the diamond surface could reconstruct to form a surface defect or react with a gas phase species other than H, e.g., C_2H, to form a surface adduct. Either of these two rare events would produce a change of surface structure which might initiate the renucleation of a nanocrystal with a different orientation from that of its parent. However, there are very few measurements of the concentrations of C_1 species in these plasmas, and so we would encourage suitable experiments (such as cavity ring down spectroscopy) to be performed to get quantitative data for CH and CH_2 in order to ascertain the veracity of this model. Atomic C is especially difficult to probe in these types of plasma environments, and so special detection methods such as a laser induced fluorescence scheme, either by one-photon vacuum UV excitation or two-photon excitation in the UV, may need to be developed if we are experimentally to verify the model predictions.

We also considered a number of other possible mechanisms for renucleation. The excess H atom concentration near the surface was ruled out as a cause for creation of large numbers of open sites since the surface open site concentration has already reached saturation at ~12%. The creation of excess open sites by Ar^* metastables, thermal Ar^+, ArH^+ ions, and excited H atoms were also ruled out due their low concentration at the substrate surface.

C_2 insertion reactions are predicted to be far more favorable on certain diamond lattice planes than others, and so should produce preferentially oriented large grains. The same is probably true for C_2H insertion reactions, although no work has yet been reported on this. Experimentally, UNCD grains are spherical and nonoriented, with a surface mostly composed of randomly arranged steps and edges; so this suggests that insertion reactions are not significant causes of growth and/or renucleation. However, the C_2H radical is an obvious candidate for more work, since it is an abundant species in the plasma and virtually no experimental measurements have been made on this radical under CVD conditions.

Calculations show that the higher concentration of C_xH_y radicals close to the surface serve to inhibit the β-scission reactions, and thereby greatly increase the fraction of long-chained hydrocarbons that are attached to the surface. The fractional coverage is sufficiently high to provide a plausible mechanism by which the diamond growth can be perturbed to initiate a nucleation site.

Accurate measurements of electrical characteristics of the plasma, especially the sheath potential and electron and ion temperatures, are also needed to confirm whether ion bombardment is, as expected, insignificant on nominally unbiased substrates at these process pressures. Much more work is needed on depositing UNCD using "ion-free" hot filament reactors, since a conclusive evidence that this can be done would rule out ion bombardment as a major cause of renucleation.

The thermodynamic stability of nanograins is an intriguing argument for the observed size distribution of UNCD films, but it is inconsistent with a number of experimental observations of film growth and therefore cannot be the "whole story."

Based on the above considerations, we propose that the most likely causes for the renucleation required for the UNCD growth are (i) the attachment of C_1 species (especially C atoms) followed by local surface restructuring, (ii) the reduction of the efficiency of the β-scission reaction, creating an increase in the number of long-chained hydrocarbons on the surface, or (iii) a combination of these two processes.

But it must be emphasised that many of the rate constants and assumptions used in the above calculations have been estimated, since actual data for the required reactions on diamond surfaces are not available. Should more reliable data become available in the future, it would be worthwhile to reevaluate some of the alternative mechanisms that we have discounted to ensure that our approximations are valid.

[1] P. W. May, Philos. Trans. R. Soc. London, Ser. A **358**, 473 (2000).
[2] C. A. Rego, P. W. May, C. R. Henderson, M. N. R. Ashfold, K. N. Rosser, and N. M. Everitt, Diamond Relat. Mater. **4**, 770 (1995).
[3] S. M. Leeds, P. W. May, E. Bartlett, M. N. R. Ashfold, and K. N. Rosser, Diamond Relat. Mater. **8**, 1377 (1999).
[4] P. K. Bachmann, D. Leers, and H. Lydtin, Diamond Relat. Mater. **1**, 1 (1991).
[5] S. J. Harris, Appl. Phys. Lett. **56**, 2298 (1990).
[6] D. G. Goodwin and J. E. Butler, in *Handbook of Industrial Diamonds and Diamond Films*, edited by M. A. Prelas, G. Popovici, and L. K. Bigelow (Marcel Dekker, New York, 1998).
[7] X. Xiao, J. Birrell, J. E. Gerbi, O. Auciello, and J. A. Carlisle, J. Appl. Phys. **96**, 2232 (2004).
[8] J. Birrell, J. E. Gerbi, O. Auciello, J. M. Gibson, D. M. Gruen, and J. A. Carlisle, J. Appl. Phys. **93**, 5606 (2003).
[9] D. Zhou, T. G. McCauley, L. C. Qin, A. R. Krauss, and D. M. Gruen, J. Appl. Phys. **83**, 540 (1998).
[10] E. Crichton and P. W. May, Proceedings of the *ICNDST-9*, Tokyo, April 2004.
[11] J. R. Rabeau, P. John, J. I. B. Wilson, and Y. Fan, J. Appl. Phys. **96**, 6724 (2004).
[12] D. M. Gruen, S. Liu, A. R. Krauss, J. Luo, and X. Pan, Appl. Phys. Lett. **64**, 1502 (1994).
[13] J. Birrell, J. E. Gerbi, O. Auciello, J. M. Gibson, J. Johnson, and J. A. Carlisle, Diamond Relat. Mater. **14**, 86 (2005).
[14] D. Zhou, D. M. Gruen, L. C. Qin, T. G. McCauley, and A. R. Krauss, J. Appl. Phys. **84**, 1981 (1998).
[15] Y. K. Liu, Y. Tzeng, C. Liu, P. Tso, and I. N. Lin, Diamond Relat. Mater. **13**, 1859 (2004).
[16] A. N. Goyette, J. E. Lawler, L. W. Anderson, D. M. Gruen, T. G. McCau-

ley, D. Zhou, and A. R. Krauss, J. Phys. D **31**, 1975 (1998).

[17]G. Lombardi, K. Hassouni, F. Bénédic, F. Mohasseb, J. Röpcke, and A. Gicquel, J. Appl. Phys. **96**, 6739 (2004).

[18]Y. A. Mankelevich, A. T. Rakhimov, and N. V. Suetin, Diamond Relat. Mater. **7**, 1133 (1998).

[19]Yu. A. Mankelevich *et al.* (unpublished).

[20]A. G. Engelhardt and A. V. Phelps, Phys. Rev. **131**, 2115 (1963); A. V. Phelps, JILA Information Center Report No. N28, 1985 (unpublished) .

[21]C. J. Rennick, R. Engeln, J. A. Smith, A. J. Orr-Ewing, M. N. R. Ashfold, and Yu. Mankelevich, J. Appl. Phys. **97**, 113306 (2005).

[22]M. N. R. Ashfold *et al.* (unpublished).

[23]G. P. Smith *et al.*, http://www.me. berkeley.edu/gri-mech/

[24]J. R. Petherbridge, P. W. May, S. R. J. Pearce, K. N. Rosser, and M. N. R. Ashfold, J. Appl. Phys. **89**, 1484 (2001), and references therein.

[25]Y. A. Mankelevich, N. V. Suetin, M. N. R. Ashfold, W. E. Boxford, A. J. Orr-Ewing, J. A. Smith, and J. B. Wills, Diamond Relat. Mater. **12**, 383 (2003).

[26]L. V. Krasnoperov, I. J. Kalinovski, H.-N. Chu, and D. Gutman, J. Phys. Chem. **97**, 11787 (1993).

[27]P. W. May, J. A. Smith, and Yu. A. Mankelevich, Diamond Relat. Mater. **15**, 345 (2006).

[28]T. Lin, Y. Yu, A. T. S. Wee, Z. X. Shen, and K. P. Loh, Appl. Phys. Lett. **77**, 2692 (2000).

[29]J. E. Butler and D. G. Goodwin, in *Properties, Growth and Applications of Diamond*, edited by M. H. Nazare and A. J. Neves (INSPEC, IEE, London, UK, 2001), Chap. B1.3.

[30]S. Skokov, B. Weiner, and M. Frenklach, J. Phys. Chem. **98**, 7073 (1994).

[31]See, e.g., J. E. Velazco, J. H. Kolts, and D. W. Setser, J. Chem. Phys. **69**, 4357 (1978); J. L. Jauberteau, L. Thomas, J. Aubreton, I. Jauberteau, and A. Catherinot, Plasma Chem. Plasma Process. **18**, 137 (1998); N. Sadeghi, D. W. Setser, A. Francis, U. Czarnetzki, and H. F. Döbele, J. Chem. Phys. **115**, 3144 (2001).

[32]W. B. Maier, J. Chem. Phys. **42**, 1790 (1965).

[33]H. Villinger, J. H. Futrell, F. Howorka, N. Duric, and W. Lindinger, J. Chem. Phys. **76**, 3529 (1982).

[34]D. A. Horner, L. A. Curtiss, and D. M. Gruen, Chem. Phys. Lett. **233**, 243 (1995).

[35]P. C. Redfern, D. A. Horner, L. A. Curtiss, and D. M. Gruen, J. Phys. Chem. **100**, 11654 (1996).

[36]M. Sternberg, M. Kaukonen, R. M. Nieminen, and Th. Frauenheim, Phys. Rev. B **63**, 165414 (2001).

[37]M. Sternberg, P. Zapol, and L. A. Curtiss, Phys. Rev. B **68**, 205330 (2003).

[38]A. C. Ferrari and J. Robertson, Phys. Rev. B **63**, 121405 (2001).

[39]V. Grill, J. Shen, C. Evans, and R. G. Cooks, Rev. Sci. Instrum. **72**, 3149 (2001).

[40]T. Sharda, T. Soga, T. Jimbo, and M. Umeno, Diamond Relat. Mater. **10**, 1592 (2001).

[41]B. N. Chapman, *Glow Discharge Processes* (Wiley, New York, 1980).

[42]J. Y. Raty and G. Galli, Nat. Mater. **2**, 792 (2003).

[43]J. Y. Raty, G. Galli, A. van Buuren, and L. Terminello, Phys. Rev. Lett. **90**, 037401 (2003).